

**Update on the recent progress of the CUORE experiment
(Proceedings of the Neutrino 2018 Conference)**

D. Q. Adams,¹ C. Alduino,¹ K. Alfonso,² F. T. Avignone III,¹ O. Azzolini,³ G. Bari,⁴ F. Bellini,^{5,6} G. Benato,⁷ A. Bersani,⁸ M. Biassoni,⁹ A. Branca,^{10,11} C. Brofferio,^{12,9} C. Bucci,¹³ A. Caminata,⁸ A. Campani,^{14,8} L. Canonica,^{15,13} X. G. Cao,¹⁶ S. Capelli,^{12,9} L. Cappelli,^{13,7,17} L. Cardani,⁶ P. Carniti,^{12,9} N. Casali,⁶ L. Cassina,^{12,9} D. Chiesa,^{12,9} N. Chott,¹ M. Clemenza,^{12,9} S. Copello,^{18,13} C. Cosmelli,^{5,6} O. Cremonesi,⁹ R. J. Creswick,¹ J. S. Cushman,¹⁹ A. D'Addabbo,¹³ D. D'Aguzzo,^{13,20} I. Dafinei,⁶ C. J. Davis,¹⁹ S. Dell'Oro,²¹ M. M. Deninno,⁴ S. Di Domizio,^{14,8} V. Dompè,^{13,18} A. Drobizhev,^{7,17} D. Q. Fang,¹⁶ M. Faverrani,^{12,9} E. Ferri,^{12,9} F. Ferroni,^{5,6} E. Fiorini,^{9,12} M. A. Franceschi,²² S. J. Freedman,^{17,7,*} B. K. Fujikawa,¹⁷ A. Giachero,^{12,9} L. Gironi,^{12,9} A. Giuliani,²³ L. Gladstone,¹⁵ P. Gorla,¹³ C. Gotti,^{12,9} T. D. Gutierrez,²⁴ K. Han,²⁵ K. M. Heeger,¹⁹ R. Hennings-Yeomans,^{7,17} R. G. Huang,⁷ H. Z. Huang,² J. Johnston,¹⁵ G. Keppel,³ Yu. G. Kolomensky,^{7,17} A. Leder,¹⁵ C. Ligi,²² Y. G. Ma,¹⁶ L. Marini,^{7,17} M. Martinez,^{5,6,26} R. H. Maruyama,¹⁹ Y. Mei,¹⁷ N. Moggi,^{27,4} S. Morganti,⁶ S. S. Nagorny,^{13,18} T. Napolitano,²² M. Nastasi,^{12,9} C. Nones,²⁸ E. B. Norman,^{29,30} V. Novati,²³ A. Nucciotti,^{12,9} I. Nutini,^{13,18} T. O'Donnell,²¹ J. L. Ouellet,¹⁵ C. E. Pagliarone,^{13,20} M. Pallavicini,^{14,8} V. Palmieri,^{3,*} L. Pattavina,¹³ M. Pavan,^{12,9} G. Pessina,⁹ C. Pira,³ S. Pirro,¹³ S. Pozzi,^{12,9} E. Previtali,⁹ A. Puii,^{12,9} F. Reindl,⁶ C. Rosenfeld,¹ C. Rusconi,^{1,13} M. Sakai,² S. Sangiorgio,²⁹ D. Santone,^{13,31} B. Schmidt,¹⁷ N. D. Scielzo,²⁹ V. Singh,⁷ M. Sisti,^{12,9} D. Speller,¹⁹ L. Taffarello,¹⁰ F. Terranova,^{12,9} C. Tomei,⁶ M. Vignati,⁶ S. L. Wagaarachchi,^{7,17} B. S. Wang,^{29,30} H. W. Wang,¹⁶ B. Welliver,¹⁷ J. Wilson,¹ K. Wilson,¹ L. A. Winslow,¹⁵ T. Wise,^{19,32} L. Zanotti,^{12,9} G. Q. Zhang,¹⁶ S. Zimmermann,³³ and S. Zucchelli^{27,4}

¹*Department of Physics and Astronomy, University of South Carolina, Columbia, SC 29208, USA*

²*Department of Physics and Astronomy, University of California, Los Angeles, CA 90095, USA*

³*INFN – Laboratori Nazionali di Legnaro, Legnaro (Padova) I-35020, Italy*

⁴*INFN – Sezione di Bologna, Bologna I-40127, Italy*

⁵*Dipartimento di Fisica, Sapienza Università di Roma, Roma I-00185, Italy*

⁶*INFN – Sezione di Roma, Roma I-00185, Italy*

⁷*Department of Physics, University of California, Berkeley, CA 94720, USA*

⁸*INFN – Sezione di Genova, Genova I-16146, Italy*

⁹*INFN – Sezione di Milano Bicocca, Milano I-20126, Italy*

¹⁰*INFN – Sezione di Padova, Padova I-35131, Italy*

¹¹*Dipartimento di Fisica e Astronomia, Università di Padova, I-35131 Padova, Italy*

¹²*Dipartimento di Fisica, Università di Milano-Bicocca, Milano I-20126, Italy*

¹³*INFN – Laboratori Nazionali del Gran Sasso, Assergi (L'Aquila) I-67100, Italy*

¹⁴*Dipartimento di Fisica, Università di Genova, Genova I-16146, Italy*

¹⁵*Massachusetts Institute of Technology, Cambridge, MA 02139, USA*

¹⁶*Shanghai Institute of Applied Physics, Chinese Academy of Sciences, Shanghai 201800, China*

¹⁷*Nuclear Science Division, Lawrence Berkeley National Laboratory, Berkeley, CA 94720, USA*

¹⁸*INFN – Gran Sasso Science Institute, L'Aquila I-67100, Italy*

¹⁹*Wright Laboratory, Department of Physics, Yale University, New Haven, CT 06520, USA*

²⁰*Dipartimento di Ingegneria Civile e Meccanica,*

Università degli Studi di Cassino e del Lazio Meridionale, Cassino I-03043, Italy

²¹*Center for Neutrino Physics, Virginia Polytechnic Institute and State University, Blacksburg, Virginia 24061, USA*

²²*INFN – Laboratori Nazionali di Frascati, Frascati (Roma) I-00044, Italy*

²³*CSNSM, Univ. Paris-Sud, CNRS/IN2P3, Université Paris-Saclay, 91405 Orsay, France*

²⁴*Physics Department, California Polytechnic State University, San Luis Obispo, CA 93407, USA*

²⁵*INPAC and School of Physics and Astronomy,*

Shanghai Jiao Tong University; Shanghai Laboratory for Particle Physics and Cosmology, Shanghai 200240, China

²⁶*Laboratorio de Fisica Nuclear y Astroparticulas,*

Universidad de Zaragoza, Zaragoza 50009, Spain

²⁷*Dipartimento di Fisica e Astronomia, Alma Mater Studiorum – Università di Bologna, Bologna I-40127, Italy*

²⁸*Service de Physique des Particules, CEA / Saclay, 91191 Gif-sur-Yvette, France*

²⁹*Lawrence Livermore National Laboratory, Livermore, CA 94550, USA*

³⁰*Department of Nuclear Engineering, University of California, Berkeley, CA 94720, USA*

³¹*Dipartimento di Scienze Fisiche e Chimiche, Università dell'Aquila, L'Aquila I-67100, Italy*

³²*Department of Physics, University of Wisconsin, Madison, WI 53706, USA*

³³*Engineering Division, Lawrence Berkeley National Laboratory, Berkeley, CA 94720, USA*

(Dated: August 27, 2018)

CUORE is a 741 kg array of 988 TeO₂ bolometric crystals designed to search for the neutrinoless double beta decay of ¹³⁰Te and other rare processes. CUORE has been taking data since summer 2017, and as of summer 2018 collected a total of 86.3 kg · yr of TeO₂ exposure. Based on this exposure, we were able to set a limit on the $0\nu\beta\beta$ decay half-life of ¹³⁰Te of $T_{1/2}^{0\nu} > 1.5 \times 10^{25}$ yr at 90% C.L. At this conference, we showed the decomposition of the CUORE background and were able to extract a ¹³⁰Te $2\nu\beta\beta$ half-life of $T_{1/2}^{2\nu} = [7.9 \pm 0.1 \text{ (stat.)} \pm 0.2 \text{ (syst.)}] \times 10^{20}$ yr. This is the most precise measurement of this half-life and is consistent with previous measurements.

INTRODUCTION

In the early 2000s, the discovery of neutrino oscillations demonstrated conclusively that neutrinos are massive particles [1–6]. But despite the nearly 20 years that have passed since this discovery, the scale and nature of that mass has still not been established. Whether the neutrino has a Dirac type mass or a Majorana type mass is one of the most actively sought questions in particle physics today. A Majorana type mass would indicate the violation of lepton number, create a natural explanation for the neutrino’s lightness, point towards new physics well beyond the scale of today’s accelerators, and would even have implications for the formation of the matter asymmetry of the universe.

The Cryogenic Underground Observatory for Rare Events (CUORE) is primarily a search for the Neutrinoless Double Beta decay ($0\nu\beta\beta$ decay) of ¹³⁰Te \rightarrow ¹³⁰Xe + 2e⁻ [7]. The discovery of this decay would indicate conclusively that the neutrino is a Majorana fermion. CUORE builds on a long history of cryogenic searches for the $0\nu\beta\beta$ decay of ¹³⁰Te [8–12] and is the first such experiment to reach the ton scale. The search for $0\nu\beta\beta$ decay is a very active area of research, with multiple experiments searching in a variety of candidate isotopes using a range of detector technologies [13–15].

The CUORE detector is an array of 988 bolometers operating independently, with each bolometer acting as an individual search for $0\nu\beta\beta$ decay. A CUORE bolometer is composed of two main components, an absorber which absorbs the energy released in a particle interaction and converts that energy into an increase in temperature and a thermistor which converts this change in temperature into a measurable change in voltage (see Fig. 1(b)). A CUORE absorber is a TeO₂ crystal, 5×5×5 cm³ in size and weighing approximately 750 g. The crystal is made using ^{nat}Te, which is ~34% ¹³⁰Te, and thus acts as both the source and detector of the decays of interest. When the decay occurs, the emitted electrons deposit their energy into the crystal lattice in the form of heat and any energy imparted to neutrinos is lost to the detector. Since no neutrinos are produced in $0\nu\beta\beta$ decay, the signal that we are searching for is a narrow peak at the full energy of the ¹³⁰Te decay, $Q_{\beta\beta} = 2527.5$ keV.

The CUORE crystals are arranged into an array of 19 towers, 13 floors each, with 4 crystals per floor (Fig. 1(a)). Each crystal has a mass of ~750 g, giving the CUORE

detector a total active mass of 741 kg, of which ~206 kg is ¹³⁰Te. This source = detector configuration gives us a high signal efficiency of around $\gtrsim 85\%$. The detector is cooled to its operating temperature of ~10 mK in the CUORE cryostat (Fig. 1(c)). At this low temperature, the heat capacity of a crystal falls to the point that a 1 MeV energy deposition causes a change in temperature of about 100 μK. This small change in temperature is read out using a neutron transmutation doped thermistor (NTD) with a resistivity that is exponentially dependent on temperature and amplifies the ~1% temperature change to a change in resistivity of ~10%. The NTDs have typical resistances of ~0.1 – 1 GΩ and are current biased and read out using room temperature electronics.

BACKGROUND REDUCTION

The figure of merit that determines the CUORE sensitivity to $0\nu\beta\beta$ decay can be expressed as $\propto \varepsilon \sqrt{MT/(b\Delta E)}$ [16], where ε is the total signal efficiency, M is the active mass, T the total detector live time, and ΔE and b are the energy resolution in keV and background in counts/(keV · kg · yr) at $Q_{\beta\beta}$. CUORE typically aims for an energy resolution of about $\Delta E \approx 5$ keV full-width half-max (FWHM) at $Q_{\beta\beta}$.

The sensitivity to $0\nu\beta\beta$ decay is thus driven by the background index, b , and a lot of work has been done over the years to improve it. The primary backgrounds in CUORE come from naturally occurring radioactivity that originates on or near materials close to our bolometers. The predecessor to CUORE, called Cuoricino [10–12], had a background index of $b = 0.169 \pm 0.006$ counts/(keV · kg · yr), of which, 0.110 ± 0.001 counts/(keV · kg · yr) came from α particles originating on surfaces of the bolometers or materials immediately facing the bolometers. The remaining background came from γ -rays originating in materials around the detector (but necessarily immediately facing it). Cuoricino ran from 2003 – 2008 and with 19.75 kg · yr of ¹³⁰Te exposure was able to set a limit on the $0\nu\beta\beta$ decay half-life of ¹³⁰Te of $T_{1/2}^{0\nu} > 2.8 \times 10^{24}$ yr at 90% C.L.

The first phase of CUORE was a single tower experiment called CUORE-0 [17, 18] operated in the same cryostat that housed Cuoricino. CUORE-0 was designed to be a full scale test of the new surface cleaning and detector assembly procedures developed to reduce the α -

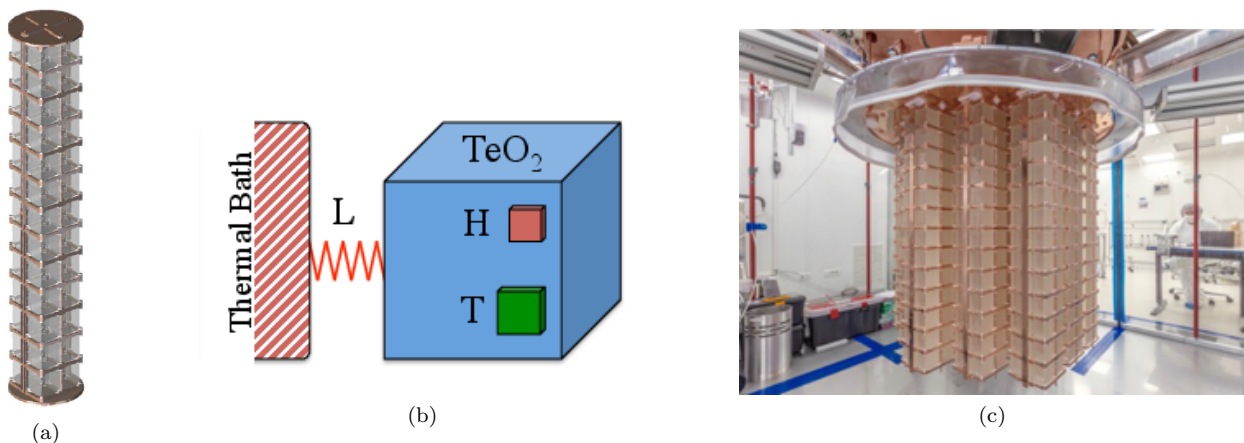


FIG. 1. (a) Schematic of a single CUORE-like tower, with 13 floors of 4 crystals each. Each tower has 52 crystals for a total mass of ~ 39 kg of TeO_2 or ~ 10.8 kg of ^{130}Te . The CUORE detector is composed of 19 such towers. (b) A schematic of a CUORE bolometer. The TeO_2 crystal acts as the absorber, and is connected to a heat bath through a weak thermal link, L . Each bolometer is instrumented with an NTD thermistor, T , and a heater to inject heat pulses, H . (c) The CUORE detector assembled and installed in the CUORE cryostat, inside the CUORE cleanroom.

background observed in Cuoricino [19, 20]. CUORE-0 was able to achieve a background index at $Q_{\beta\beta}$ of $b = 0.058 \pm 0.004(\text{stat.}) \pm 0.002(\text{syst.})$ counts/(keV \cdot kg \cdot yr) with only 0.016 ± 0.001 counts/(keV \cdot kg \cdot yr) coming from α -backgrounds. The γ -background was observed to be consistent with Cuoricino as was anticipated since the γ backgrounds were believed to originate in the materials of the cryostat, which was common to both experiments. CUORE-0 ran from 2013 – 2015 and collected an exposure of 9.8 kg \cdot yr of ^{130}Te . Using the result of Cuoricino as a prior, CUORE-0 set a limit on the $0\nu\beta\beta$ decay of ^{130}Te of $T_{1/2}^{0\nu} > 4.0 \times 10^{24}$ yr at 90% C.L. [8, 9].

CUORE uses the same surface cleaning and assembly procedure as CUORE-0 and aims to achieve a background at $Q_{\beta\beta}$ of $b = 0.01$ counts/(keV \cdot kg \cdot yr) [21]. The reduction in α -background was mostly demonstrated in CUORE-0, with the remaining reduction coming from the larger volume-to-surface ratio of CUORE. The γ -background is reduced to a subdominant level by the cleaner materials used to build the CUORE cryostat, as well as the improved shielded and better anti-coincidence capabilities of a larger detector.

CUORE DATA TAKING

The CUORE detector completed assembly in summer 2014 and commissioning of the CUORE cryostat completed two years later in summer of 2016. The detector was then installed into the cryostat inside a specially built anti-radon tent; this minimized the exposure to radon during the installation process[23]. The first CUORE cooldown started in December 2016 and reached base temperature in January 2017.

After a period of detector commissioning, CUORE collected its first two datasets in the summer of 2017. This data comprised a total of 86.3 kg \cdot yr of TeO_2 exposure (24.0 kg \cdot yr of ^{130}Te exposure) characterized by an effective energy resolution of $\Delta E = 7.7 \pm 0.5$ keV FWHM (see Fig. 2(a)) and a background index at $Q_{\beta\beta}$ of $b = 0.014 \pm 0.002$ counts/(keV \cdot kg \cdot yr). The background index is slightly higher than our background goal of 0.01 counts/(keV \cdot kg \cdot yr) in part because we have not yet implemented all of the data quality cuts at our disposal. The energy resolution is also larger than our goal of 5 keV FWHM. However, between the two datasets presented here, we improved the energy resolution from 8.3 keV to 7.4 keV and we aim to continue to improve the resolution as we continue to develop better algorithms as well as a better understanding of the new CUORE cryostat.

The summed spectrum from the first two datasets can be seen in Fig. 3 compared with the spectrum observed in CUORE-0. Overall, the observed CUORE spectrum was consistent with our expectations. We saw a significant decrease in the γ -background ($\lesssim 3$ MeV) relative to CUORE-0. This is due to the significantly improved material selection and shielding of the CUORE cryostat. The α -region ($\gtrsim 3$ MeV) is consistent with what we observed in CUORE-0. This was expected as CUORE-0 and CUORE shared the same surface cleaning and assembly procedures. We do observe one unexpected background which is an excess of surface ^{210}Po events near 5.4 MeV. The source of this background is still unexplained, but the contamination appears to be a very shallow surface contamination very close to the bolometers. This contamination does not appear to significantly increase the background in the $0\nu\beta\beta$ decay ROI (see

MEASUREMENT OF THE $2\nu\beta\beta$ DECAY HALF-LIFE

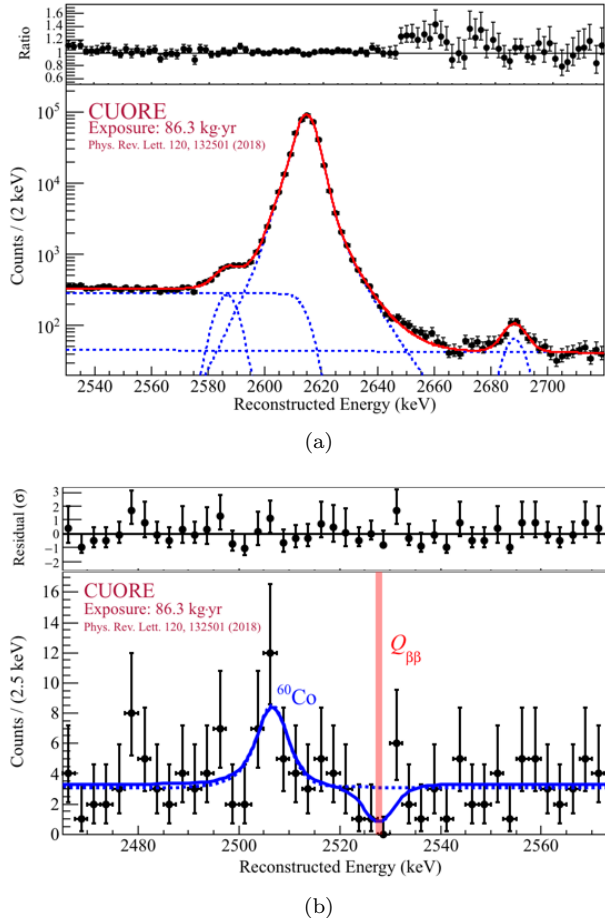


FIG. 2. (a) Reconstructed ^{208}Tl 2516 keV in the calibration spectrum. *Lower*: The black points are data and the red line is the reconstructed line shape. The dotted blue lines are the components of the line shape corresponding to different physical processes (e.g. full energy deposition, low angle Compton-scattering, X-ray escape, etc.). (b) The best fit in the ROI, with the expected $Q_{\beta\beta}$ value at 2527.518 keV marked. Both plots taken from [22].

Fig. 3).

With the first two datasets, CUORE was able to set a limit on the $0\nu\beta\beta$ decay half-life of ^{130}Te of $T_{1/2}^{0\nu} > 1.3 \times 10^{25}$ yr. This result outperforms the expected half-life sensitivity of 7.6×10^{24} yr due to a $\sim 2\sigma$ -downward fluctuation in the background right at $Q_{\beta\beta}$. When combined with the results of CUORE-0 and Cuoricino, we set the most stringent limit on the $0\nu\beta\beta$ decay half-life of ^{130}Te to date at $T_{1/2}^{0\nu} > 1.5 \times 10^{25}$ yr at 90% C.L. [22]. The ultimate sensitivity of CUORE after 5 years of live time is 9×10^{25} yr.

In order to understand the observed CUORE spectrum, we simulate many possible background sources with a GEANT4 [24] Monte Carlo (MC) simulation. These backgrounds include surface contaminations of the materials near to our bolometers, bulk contaminations of materials both near and far from our bolometers, and cosmogenic muons. More information about the CUORE MC simulation can be found in [21, 25].

We split the data into three types of spectra: a multiplicity 1 (M1) spectrum comprised of events where energy was deposited into a single bolometer, a multiplicity 2 (M2) spectrum comprised of the single bolometer energies of events where energy was shared between two bolometers, and an M2 sum spectrum ($\Sigma 2$) comprised of the summed energy of the M2 events. Double beta decay events deposit all of their energy into a single bolometer about 90% of the time and so are primarily in the M1 spectrum, whereas many of our backgrounds deposit energy across two or more bolometers (e.g. γ -rays that scatter from one crystal into another or α -decays that occur on a surface between two neighboring crystals.) So the M2 and $\Sigma 2$ spectra are particularly useful for understanding our backgrounds (see Fig. 4). The M1 spectrum is further split into two independent spectra: the layer 0 spectrum (M1L0) which is comprised of the 252 “inner core” bolometers, which are expected to be more shielded from external backgrounds; and the layer 1 spectrum (M1L1) comprised of the 736 bolometers on the surface of the detector, which are expected to be more susceptible to backgrounds originating outside the detector.

We then reconstruct the observed CUORE background by fitting the MC simulated spectra to the observed data simultaneously across these four spectra using a Markov-Chain Monte Carlo (MCMC) implemented in the JAGS software package [26–28]. The fit has a total of 60 free parameters corresponding to the contamination levels of each background component. Both the observed and MC spectra are binned with variable bin sizes to reduce the effect of the complicated line shapes. The fitting procedure closely follows the procedure laid out in [25] and a paper describing the precise procedure for CUORE is in preparation.

Overall the model is able to reproduce nearly all of the major features of the observed spectra (see Fig. 5). The χ^2 values are reported in Table I, and show reasonable agreement between the fit and the data. Much of the disagreement between the data and reconstruction comes from a poor reconstruction of several α and γ peaks which – due to the high statistics of the peaks – have a large effect on the χ^2 . But practically, these indicate that we have not yet properly modeled all the contaminations leading to these backgrounds. In the future, effects such

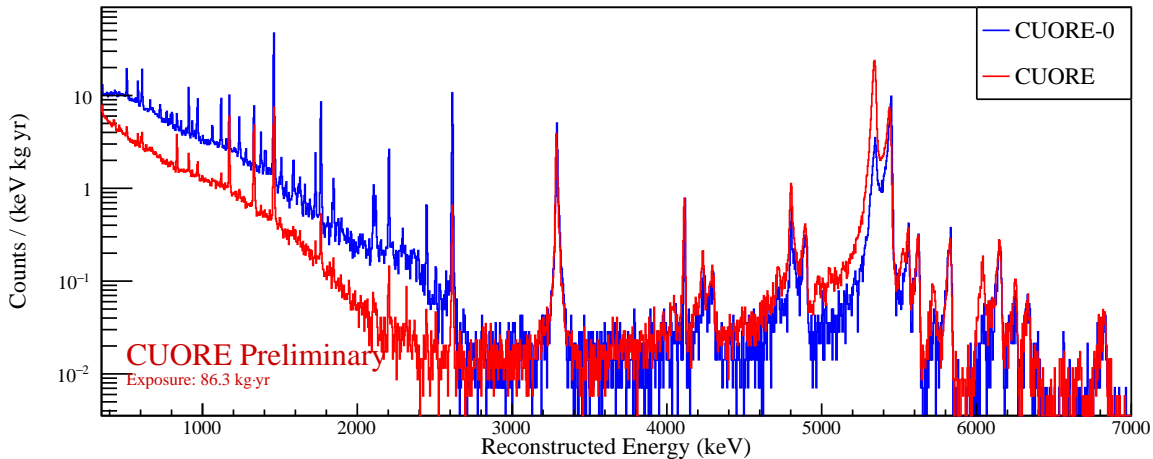


FIG. 3. The observed CUORE M1 spectrum (*red*) vs the CUORE-0 M1 spectrum (*blue*). We see a significant decrease in the observed rate in the γ -region (below 3 MeV). The α -region (above 3 MeV) is consistent with what was observed in CUORE-0. The excess of ^{210}Po surface events can be seen as the larger peak near 5.3 MeV in the CUORE spectrum. However, this does not appear to increase the background in the $0\nu\beta\beta$ decay ROI, as can be seen by the agreement of the backgrounds around 3 MeV.

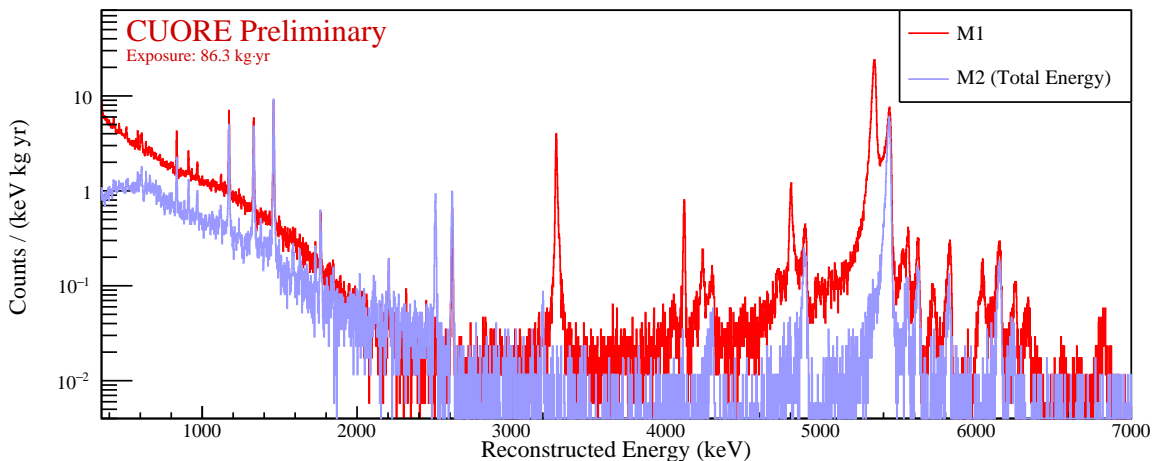


FIG. 4. The CUORE M1 spectrum vs the $\Sigma 2$ spectrum. The $\Sigma 2$ spectrum is more sensitive to γ events and surface α events. We can see this by the lack of double peaks in the α -region, since for an M2 event, the α and recoiling nucleus must both be detected. The peak at ~ 3.2 MeV corresponds to the α -decay of ^{190}Pt , which is a bulk contamination of the TeO_2 crystal from its growing procedure. Since the ^{190}Pt is in the crystal bulk, the full energy is typically contained in the originating crystal and the peak only appears in the M1 spectrum.

as these will improve with increased statistics as we are able to disentangle the origins of the contaminations.

The remaining systematic effects create a very large uncertainty in the background rate in the $0\nu\beta\beta$ decay region of interest (ROI) around $Q_{\beta\beta}$. As such, we leave a measurement of the background index and its effect on the sensitivity of CUORE to $0\nu\beta\beta$ decay for future work.

Despite these systematic uncertainties, we are able to extract a robust estimate of the $2\nu\beta\beta$ half-life. Due to the very low γ -backgrounds and increased ^{130}Te mass of CUORE, the $2\nu\beta\beta$ decay is the dominant component of

the observed M1 spectrum from about 1 - 2 MeV (see Fig. 6). To prevent bias while tuning our data quality cuts and fitting procedure, we blinded our MC normalization constant to keep the extracted half-life in terms of an unphysical ratio that could not be compared to previous results. When the fit procedure was finalized, we unblinded the correct normalization and extracted a measurement of the $2\nu\beta\beta$ half-life of ^{130}Te of $T_{1/2}^{2\nu} = [7.9 \pm 0.1 (\text{stat.}) \pm 0.2 (\text{syst.})] \times 10^{20}$ yr. This result is consistent with previous measurements of this half-life (see Table II). The present result represents the most

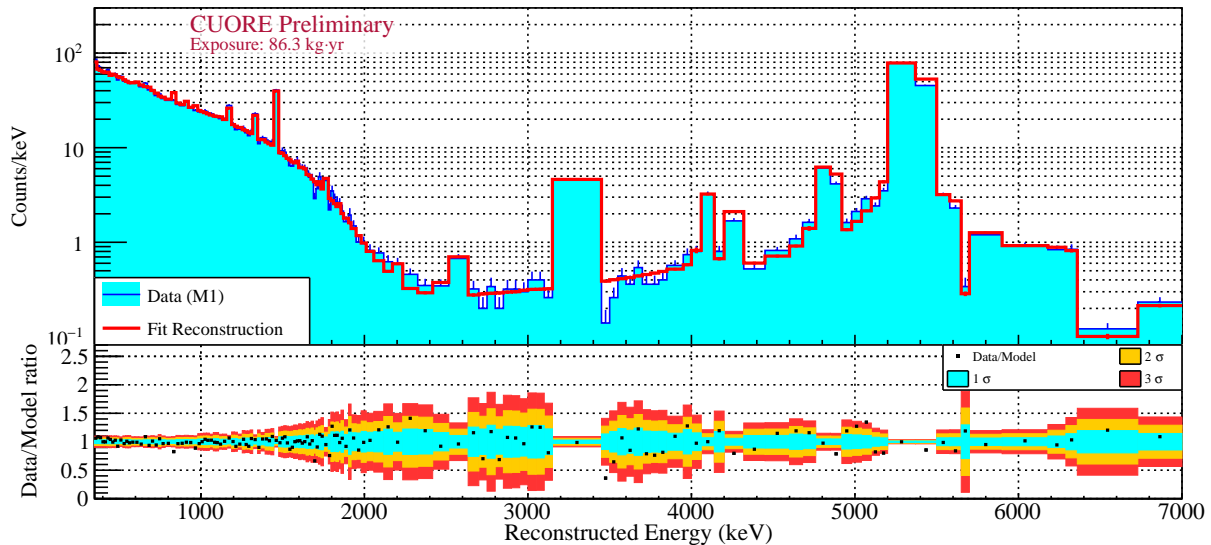


FIG. 5. Top: The measured M1L0 spectrum (*blue*) and its reconstruction (*red*). The spectra are binned with an adaptive binning to contain peaks into a single bin (to avoid dependence on the peak shape), while also achieving good resolution of the continuum shape. Bottom: The ratio of the data to the reconstructed model with 1σ , 2σ and 3σ error bars. It is clear from the data that we are able to faithfully reconstruct the continuum, with moderate disagreement in the heights of a few peaks.

TABLE I. Table of fit χ^2 values for the four spectra, along with the associated number of degrees of freedom.

	χ^2	d.o.f.	χ^2_{red}
M1L0	388.5	139	2.80
M1L1	387.5	158	2.20
M2	408.5	130	3.15
$\Sigma 2$	273.9	102	2.69
Total	1418.7	529	2.68

TABLE II. Recent measurements of the $T_{1/2}^{2\nu}$ of ^{130}Te .

	$T_{1/2}^{2\nu}$ (10^{20} yr)	Frac.Uncert.	Ref.
MiBeta	$6.1 \pm 1.4^{+2.9}_{-3.5}$	57.3%	2003 [29]
NEMO-3	$7.0 \pm 0.9 \pm 1.1$	20.3%	2011 [30]
CUORE-0	$8.2 \pm 0.2 \pm 0.6$	7.7%	2016 [25]
CUORE	$7.9 \pm 0.1 \pm 0.2$	2.8%	(this result)

precise measurement of the $2\nu\beta\beta$ half-life of ^{130}Te to date and one of the most precise measurements of a $2\nu\beta\beta$ decay half-life to date.

The only component of the reconstructed model that is strongly correlated with the $2\nu\beta\beta$ decay rate is the contamination level of ^{40}K in the TeO_2 crystal bulk (see Fig. 7). ^{40}K has a β^- -decay with a 1310.9 keV endpoint (see Fig. 6), which becomes correlated with the broad $2\nu\beta\beta$ spectrum. A similar effect was seen in CUORE-0 which had an identical crystal growth process and the same ^{40}K contamination levels. But the larger statistics of CUORE and the lower background – particularly in the 1 - 2 MeV region – makes this only a small ($\sim 1\%$)

statistical uncertainty on the final measured rate.

One of the major improvements over the first CUORE $0\nu\beta\beta$ decay result, is an improvement to the estimation of the signal acceptance efficiency. Previously, we had been using several γ lines to estimate the efficiency of good signal events passing the pulse shape cuts to contribute to the final observed spectrum. This approach was limited by statistics and had to be interpolated between γ lines and thus contributed a $\sim 2.4\%$ uncertainty to the final result. In the present analysis, we are using the M2 spectrum. Due to the very low event rate of CUORE, accidental M2 events are rare ($\lesssim 1\%$) and so the M2 spectrum constitutes a clean sample of events, distributed in energy, to test for the signal efficiency. This significantly increases the statistics relative to the previous approach and as a result decreases the uncertainty on the present signal efficiency to $\lesssim 0.2\%$.

The leading systematic uncertainty on the measurement of $T_{1/2}^{2\nu}$ is now the geometric splitting of the data into subgroups. Our fit reconstruction splits the data into an inner layer of 252 bolometers and an outer layer of 736 bolometers, however, other splittings of the data are also possible and yield different results. Other splittings include looking at only even or odd channels, even or odd towers, even or odd floors, the top half vs bottom half of the detector, etc. These different splittings of the data by geometry allow us to probe the uncertainty caused by our present ignorance of the exact origin of localized contaminations. The precise details of this procedure will be laid out in future publications.

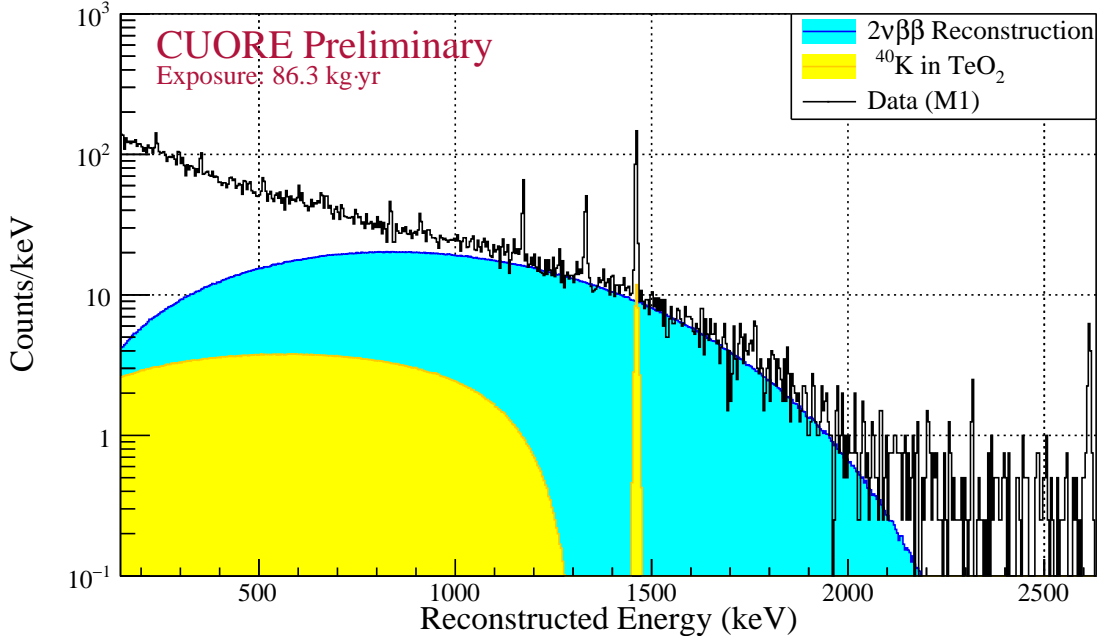


FIG. 6. The observed M1L0 spectrum (*black*) with a reconstruction of the $2\nu\beta\beta$ component (*blue*) of the background as well as the ^{40}K background (*yellow*). The $2\nu\beta\beta$ component dominates the observed M1L0 spectrum between ~ 1 to ~ 2 MeV. Note: The observed spectra has been converted back to the 1 keV binning and the $2\nu\beta\beta$ and ^{40}K to smooth continua for illustrative purposes, the fit is performed with the binning in Fig. 5.

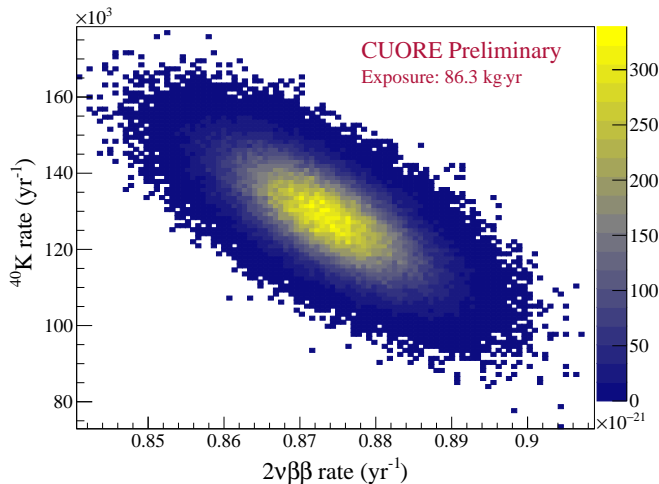


FIG. 7. The correlation between the reconstructed $2\nu\beta\beta$ decay rate, $\Gamma^{2\nu}$ and the observed ^{40}K event rate. The anti-correlation with ^{40}K in the TeO_2 bulk is the largest statistical correlation observed.

CRYOSTAT MAINTENANCE

After the two datasets collected in summer 2017, we paused data taking for a period of optimization and maintenance on the CUORE cryostat. This began with a scan

of the detector performance of a function of temperature. We measured the noise levels and energy resolution of heater pulses at operating temperatures of 11, 13, 15, 17 and 19 mK. Based on this data, we selected a new operating temperature of 11 mK, as opposed to the 15 mK at which we had previously been operating.

Starting in January 2018, we warmed the detector to 100 K to upgrade a set of vacuum gate valves. This operation was performed without fully warming to room temperature, but warm enough to allow us to overpressure the vacuum region with He gas. In total, this operation took about 2 months to complete, which is very quick given the size and cold mass of the CUORE cryostat.

We returned to base temperature in March 2018 and performed a scan of the pulse tubes to find the optimal phase configuration of the 4 CUORE pulse tubes that minimizes the noise on the detector (see [31]). In April 2018, we returned to our operating configuration and performed a detector calibration. We were able to return to our previous data taking configuration, recovering a 7.6 keV FWHM energy resolution and continue working on improve the detector operation. We resumed stable physics data taking in May 2018.

CONCLUSION

CUORE began collecting data in summer of 2017 and, with the first two datasets and an exposure of $24.0 \text{ kg} \cdot \text{yr}$ of ^{130}Te exposure, has already set the strongest limit on the $0\nu\beta\beta$ decay half-life of ^{130}Te to date at $T_{1/2}^{0\nu} > 1.5 \times 10^{25} \text{ yr}$ at 90% C.L. Recently, we have been working to reconstruct the background and were able to make a measurement of the $2\nu\beta\beta$ decay half-life of ^{130}Te of $T_{1/2}^{2\nu} = [7.9 \pm 0.1 \text{ (stat.)} \pm 0.2 \text{ (syst.)}] \times 10^{20} \text{ yr}$. This is the most precise measurement of the $2\nu\beta\beta$ decay half-life of ^{130}Te and one of the most precise measurements of any $2\nu\beta\beta$ decay to date.

In the past few months, CUORE has undergone a period of upgrades and optimization and has entered a period of stable data taking. We continue to work to improve the energy resolution to our goal of 5 keV FWHM and reach the background goal of $b = 0.01 \text{ counts}/(\text{keV} \cdot \text{kg} \cdot \text{yr})$. The ultimate sensitivity goal for CUORE is $9.0 \times 10^{25} \text{ yr}$ after 5 years of live-time.

* Deceased

- [1] S. Fukuda *et al.* (Super-Kamiokande), Phys. Lett. B **539**, 179 (2002), arXiv:hep-ex/0205075 [hep-ex].
- [2] Q. R. Ahmad *et al.* (SNO), Phys. Rev. Lett. **87**, 071301 (2001).
- [3] Q. R. Ahmad *et al.* (SNO), Phys. Rev. Lett. **89**, 011301 (2002).
- [4] K. Eguchi *et al.* (KamLAND), Phys. Rev. Lett. **90**, 021802 (2003).
- [5] A. Gando *et al.* (KamLAND), Phys. Rev. D **83**, 052002 (2011).
- [6] M. Tanabashi *et al.* (Particle Data Group), Phys. Rev. D **98**, 030001 (2018).
- [7] R. Ardito *et al.*, (2005), arXiv:hep-ex/0501010 [hep-ex].
- [8] K. Alfonso *et al.* (CUORE Collaboration), Phys. Rev. Lett. **115**, 102502 (2015).
- [9] C. Alduino *et al.* (CUORE), Phys. Rev. C **93**, 045503 (2016).
- [10] E. Andreotti *et al.* (Cuoricino Collaboration), Astropart. Phys. **34**, 822 (2011).
- [11] C. Arnaboldi *et al.* (Cuoricino Collaboration), Phys. Lett. B **584**, 260 (2004).
- [12] C. Arnaboldi *et al.* (Cuoricino Collaboration), Phys. Rev. C **78**, 035502 (2008).
- [13] M. Agostini *et al.* (GERDA Collaboration), Phys. Rev. Lett. **120**, 132503 (2018).
- [14] A. Gando *et al.* (KamLAND-Zen Collaboration), Phys. Rev. Lett. **117**, 082503 (2016).
- [15] J. B. Albert *et al.* (EXO-200 Collaboration), Phys. Rev. Lett. **120**, 072701 (2018).
- [16] C. Alduino *et al.* (CUORE), Eur. Phys. J. **C77**, 532 (2017).
- [17] C. Alduino *et al.* (CUORE), JINST **11**, P07009 (2016).
- [18] D. R. Artusa *et al.* (CUORE Collaboration), Eur. Phys. J. C **74**, 2956 (2014).
- [19] F. Alessandria *et al.* (CUORE Collaboration), Astropart. Phys. **45**, 13 (2013).
- [20] E. Buccheri *et al.*, Nucl. Instrum. Meth. **A768**, 130 (2014).
- [21] C. Alduino *et al.* (CUORE), Eur. Phys. J. **C77**, 543 (2017).
- [22] C. Alduino *et al.* (CUORE), Phys. Rev. Lett. **120**, 132501 (2018).
- [23] G. Benato *et al.*, JINST **13**, P01010 (2018).
- [24] S. Agostinelli *et al.* (GEANT4), Nucl. Instrum. Meth. **A506**, 250 (2003).
- [25] Alduino, C. *et al.* (CUORE Collaboration), Eur. Phys. J. C **77**, 13 (2017).
- [26] A. Gelman, J. B. Carlin, H. S. Stern, and D. B. Rubin, *Bayesian Data Analysis*, 2nd ed., Texts in Statistical Science (Chapman and Hall/CRC Press, Boca Raton, FL, 2014).
- [27] M. Plummer, *JAGS User's Manual* version 3.3.0 (2012).
- [28] D. Chiesa, E. Previtali, and M. Sisti, Ann. Nucl. Energy **70**, 157 (2014).
- [29] C. Arnaboldi *et al.*, Phys. Lett. B **557**, 167 (2003).
- [30] R. Arnold *et al.* (NEMO-3 Collaboration), Phys. Rev. Lett. **107**, 062504 (2011).
- [31] A. D'Addabbo *et al.*, Cryogenics **93**, 56 (2018).